Radio Recombination Lines: A New Observational Tool in Astrophysics

A new observational approach to star formation and large-scale structure of our galaxy is discussed.

P. G. Mezger and Patrick Palmer

In this article we describe the application of radio frequency spectroscopy to astronomy in order to study several phenomena ranging in scale from the excitation of atoms to the structure of the galaxy.

The spiral arms of a galaxy are made up of stars and interstellar matter, the principal constituent of which is hydrogen. The hottest, most massive stars are seen to ionize nearby matter almost completely, and these regions are called HII regions, since about 90 percent of the ions are of hydrogen. The main reason for our interest in these particular regions of interstellar space is that it is here that formation of stars has recently taken place and might still be taking place. Furthermore, optical observations of other galaxies have shown that HII regions are objects that clearly define the spiral structure of galaxies.

Unfortunately, such optical observations in our own galaxy are restricted to a relatively small region around the sun because light is greatly absorbed by interstellar matter. But electromagnetic radiation at longer wavelengths is not affected in this way. Thus it seems that radio observations of HII regions might add to our knowledge of star-formation and the large-scale structure of the galaxy. Even so, until recently the interest in galactic radio astronomy, and particularly in observations of HII regions, was declining.

Now new interest has been stimulated by (i) the detection of lines emitted by interstellar molecules of the hydroxyl radical (OH) at the 18-centimeter wavelength [reviewed recently by Barrett (*1*)], especially their nonthermal emission from clouds associated with HII regions; (ii) radio recombination lines of hydrogen, helium, and possibly carbon have been detected from HII regions; and (iii) at the same time, large radio telescopes have been successfully developed for operation at centimeter wavelengths—telescopes with angular resolution allowing the detailed investigation of the structure of HII regions and other galactic sources.

This article reports mainly on observations of radio recombination lines. However, the wealth of astrophysical information that has been gained from these observations is due at least partly to the fact that they were supplemented by both continuum observations and observations of the 21- and the 18-centimeter line radiation emitted by the H atom and the OH molecule, respectively. Therefore, observations of the radio recombination lines emitted from HII regions must be seen in the general frame of galactic astronomy. We will discuss these observations with particular emphasis on three problems that we believe radio recombination line research will contribute to significantly: (i) the microscopic physical processes taking place in interstellar matter, (ii) the evolution of HII regions and the determination of their macroscopic internal parameters, and (iii) the large-scale structure of our galaxy.

Formation of HII Regions and Stars

An HII region is a plasma of relatively low density (electron densities $N_e \leqq 10^4$ cm^{-3}) in which the ionization by starlight is in equilibrium with the recombination of ions with free electrons. We can distinguish two types of HII regions according to whether the size is limited by the lack of further material to be ionized or by the amount of ionizing radiation from the star. The former is called a density-bounded HII region; the latter is said to be ionization-bounded. In the latter case the transition between the fully ionized plasma and the surrounding neutral interstellar matter is very abrupt and the ionization front is well defined. In the idealized case of plasma with uniform density, the ionization front forms a "Strömgren sphere" (after the astrophysicist who pioneered the theory), and the radius of this sphere is determined by the density of the surrounding matter and the luminosity of the star.

Table 1, compiled from computations by Rubin and star parameters conforming to Hjellming and Jarecke (*2*), gives an idea of the variation of Strömgren radii for different ionizing stars and for interstellar matter with different electron densities but a constant electron temperature of 7000°K. Stars are classified according to their surface brightness. The sequence of names is O, B, A, F, G, K, M, R, N, and S, each class usually being divided continuously between 0 and 10. In Table 1 we have considered a subsequence of the most luminous and most massive stars known in our galaxy, of types O4 through B0.5. (The most luminous stars that have actually been observed are O4 stars.) Their approximate physical parameters, normalized to those of the sun, are given in columns 2 through 5. The Strömgren radii (R_s) in column 6, computed for four different densities of the plasma, are given in parsecs where 1 parsec = 3.26 light-years = 3.09×10^{18} centimeters. It requires the most massive stars to account for the Strömgren spheres of most of the observed thermal radio sources. Since an O star with a mass 30 times that of the sun has a lifetime on the main sequence of stellar evolution of only 4×10^6 years, the stars listed in Table 1 are relatively young objects compared to the age of the universe, which is greater than 5×10^9 years.

Our knowledge of the early stages of the formation of stars and HII regions is not very satisfactory from either a theoretical or an observational point of view. With these reservations, we will describe a possible history of the formation of an association of stars from a large cloud of interstellar material. Under certain conditions the

Dr. Mezger holds the position of Scientist at the National Radio Astronomy Observatory, Green Bank, West Virginia. Mr. Palmer is a graduate student in the department of physics, Harvard University, and is currently completing his thesis on radio recombination lines at Harvard College Observatory, Cambridge, Massachusetts.

Table 1. Strömgren radii of stars of early spectral type computed for different densities. Abbreviations: T_{eff}, effective star temperature; R_*/R, M_*/M, and L_*/L are the radius, mass, and luminosity of the star normalized to the radius, mass, and luminosity of the sun, respectively.

1	2	3	4	5	6a	6b	6c	6d	6e
Spectral type	T_{eff}/°K	R_*/R	M_*/M	L_*/L	Strömgren radius in parsecs for T_e = 7000°K and N_e per cm^3				
					1	10	10^2	10^3	10^4
O4	50,000	8.0	53	3.57×10^5	79.2	17.1	3.7	0.79	0.17
O5	45,000	6.8	34	1.68×10^5	59.2	12.8	2.8	.59	.13
O6	40,000	5.8	24	7.60×10^4	41.4	8.9	1.9	.41	.09
O7	38,000	5.5	22	5.63×10^4	35.1	7.6	1.6	.35	.08
O8	36,000	5.2	19	4.00×10^4	27.6	6.0	1.3	.28	.06
O9	35,000	5.0	18	3.32×10^4	23.4	5.0	1.1	.23	.05
O9.5	33,000	4.7	16	2.37×10^4	16.1	3.5	0.75	.16	.03
BO	31,000	4.5	14	1.68×10^4	10.3	2.2	.48	.10	.02
B0.5	29,000	4.4	13	1.19×10^4	6.5	1.4	.30	.06	.01

gravitational attraction within a very massive and cool cloud of interstellar material can overcome the pressure—it has become gravitationally stable—and the cloud collapses. After the density has increased sufficiently, the cloud breaks up into smaller fragments that continue to contract. The gravitational energy released during the contraction heats the center of the fragment until the temperature at the center reaches about 2×10^7°K. At this time the pressure and temperature are such that nuclear reactions begin and the first stars of the association have been formed. The most massive stars will reach the main sequence first and then will ionize the surrounding interstellar material. The size of the initial HII region (initial Strömgren sphere) depends on the spectral type (luminosity) of the star and the density of the surrounding matter. There are strong indications, based on observations, that the initial densities of young HII regions are much higher ($N_e \geqq 10^4$ cm^{-3}) than previously assumed (*3–5*). Possibly the star, after nuclear reactions begin in its core, first ionizes the outer shell of the contracting fragment, forming an ionization-limited HII region inside an optically opaque "cocoon" of dust and neutral matter (*6*). This ionized shell will expand rapidly and the density will decrease as the size of the HII region increases. The expanding ionization front will sweep around neutral regions of higher density, for example, smaller fragments of the initial collapsing cloud, and the increased outer pressure exerted by the surrounding HII region may help these fragments to contract further and form stars of smaller masses.

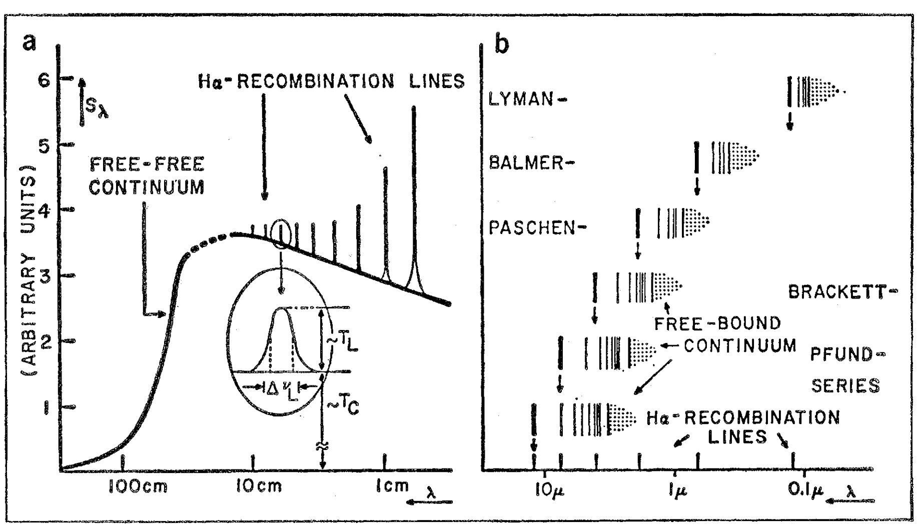

Fig. 1. (a) The radio spectrum of an HII region. The free-free continuum radiation dominates at low frequencies, but with increasing frequency the intensity of the recombination line relative to the continuum also increases. Only every tenth hydrogen (H) α-line is shown in the diagram. The spectrum is plotted as a function of wavelength (λ), which is related to frequency by the formula $\lambda \cdot \nu = c$, the speed of light. (b) In the optical part of the spectrum of an HII region the hydrogen recombination lines dominate over a weak free-bound continuum (whereas the contribution of free-free continuum is negligible). Only the first line of each series corresponds to an H*n*α-line. The strongest lines in the optical region that are emitted by trace elements, such as nitrogen, neon, and oxygen, are not shown in this diagram.

Radio Radiation from HII Regions

Both free electrons and electrons bound in atoms are the sources of electromagnetic radiation in HII regions. A free electron in an HII region can interact with one of the ions either by being recaptured or by being scattered in the ion's Coulomb field. In the latter case it loses energy that is converted into electromagnetic radiation known as bremsstrahlung. Since the initial and final energies of the electron can assume any value, the transitions are called free-free. Radiation of every frequency is emitted in this way, yielding the continuum spectrum at the radio wavelengths. At low frequencies the HII region is opaque (later referred to as optically thick). Here it radiates as a blackbody with temperature equal to the kinetic temperature of the free electrons (electron temperature, T_e). At higher frequencies the spectrum turns over and the region becomes transparent (or optically thin). In this part of the spectrum the flux emitted by the HII region decreases very slowly with frequency (Fig. 1a).

Eventually the free electron is recaptured by an ion. (The time for recapture in years is about 10^4 divided by the electron density in cubic centimeters, that is, about 10 years for a density N_e = 10^3 cm^{-3}, which illustrates the diffuseness of these objects.) The recombining electron can occupy any of the energy levels of the atom or ion, but if it is captured into a level other than the ground level it will drop to the ground level by making one transition or, more usually, a series of transitions. In this case both initial and final energies of the electron are well defined, giving the name bound-bound transition, so that the result is the emission of a spectral line. The frequency of such a line is given for large quantum numbers n and n' by the Rydberg formula:

$$\nu_L = Z^2R \left(\frac{1}{n^2} - \frac{1}{n'^2}\right) \quad (1)$$

where R is the Rydberg constant; Z, the effective nuclear charge; n, the principal quantum number of the lower energy level; and n' the principal quantum number of the upper energy level. The energy levels are populated mostly by this process of recombination and subsequent cascade toward the ground level, so that the lines have been called recombination lines.

For small values of n, recombination lines fall in the range of optical spectroscopic studies. For $n \geq 60$, transitions of types $n' = (n + 1) \rightarrow n$ (so-called α transitions) yield spectral lines whose frequencies fall in the conventional radio range ($\nu < 30$ Ghertz). The highly excited electrons that give rise to the radio recombination lines circle the nucleus in large orbits. (For $n = 100$ the radius of the orbit is, for example, larger than 0.5 microns.) Even if the nucleus is not a simple proton, as in the case of hydrogen atoms, but consists of a nucleus surrounded by one or more electrons in close orbits for these highly excited electrons, it acts as a point charge. Consequently the radio recombination spectrum of helium and heavier elements is very similar to that of the hydrogen atom, except that the rest frequencies of corresponding lines are slightly shifted toward higher frequencies. This occurs because the Rydberg constant in Eq. 1 depends on the ratio of the mass of the electron m_e to the mass of the nucleus M, $R_M = R_\infty / (1 + m_e/M)$, with R_∞ the Rydberg constant of an atom with infinitely large mass (see Table 2).

In the radio recombination spectra of hydrogen and heavier elements, we find, apart from α-transitions, lines that result from higher-order transitions. [Transitions of the type $n + 2 \rightarrow n$ are denoted by β, $n + 3 \rightarrow n$ by γ, and so on. In general, a radio recombination line is labeled by the chemical symbol of the element, followed by the principal quantum number n of the lower level, and then the Greek letter designating the change in the principal quantum number in the transition (*7*).] The H137β-line, for example, nearly coincides in frequency with the H109α-line, its predicted intensity being about 28 percent that of the H109α-line (Fig. 2).

So far radio recombination lines of the hydrogen atom have been observed in the frequency range between 8872.5 megahertz (H90α-line) and 404 megahertz (H253α-line); in addition, radio recombination lines of the helium atom and, possibly, of the carbon atom have been measured. Four basic parameters are measured in recombination line studies: T_C, the temperature of the continuum emission adjacent to the line; T_L, the excess temperature of the line above the continuum; $\Delta\nu_L$, the line width (we use the full line width at the half intensity point); $\Delta\nu$, the Doppler frequency shift of the line from its rest frequency. The first three of these quantities are indicated in Fig. 1a. When the optical depth of the continuum is small compared to unity, the observed quantities are related to the electron temperature T_e and the line frequency ν_L by

$$\Delta\nu_L \frac{T_L}{T_C} \propto \frac{\nu_L^{2.1}}{T_e^{1.15}} \quad (2)$$

[A quantitative relation between the electron temperature T_e and the observed quantities T_L, T_C, and $\Delta\nu_L$ was first given by Kardashev (*8*). More accurate formulas and discussions of the conditions of their validity are given by Hjellming *et al.* (*9*) and by Palmer (*10*).] At the "turnover" frequency below which the free-free continuum decreases, the optical depth of the continuum becomes larger than unity and the recombination lines merge with the continuum (Fig. 1a). If the width of the recombination lines is determined by Doppler broadening alone, $\Delta\nu_L$ is proportional to ν_L, and consequently the ratio of line-to-continuum brightness temperature T_L/T_C increases in proportion with the line frequency. In Fig. 1a every tenth $n\alpha$-line is shown.

Table 2. Rydberg constants and the frequencies for the 109α-lines of various elements.

Element	Rydberg constant (hertz × 10^{15})	$\nu_L(109\alpha)$
H	3.288052	5008.923
He	3.289391	5010.964
C	3.289927	5011.417
∞	3.289842	5011.644

As seen in Fig. 1a the free-free continuum radiation is dominant in the radio region of the spectrum. In the optical part of the spectrum the contribution of free-free radiation is negligible. Free-bound transitions give rise to only a weak continuum, but the recombination lines are the dominant part of the observable radiation. In Fig. 1b the optical counterparts of the radio recombination lines are shown in the well-known Lyman, Balmer, Paschen, Brackett, and so on, series. Only the first line of each series corresponds to an α-transition.

The abundance of helium in the interstellar medium is about 10 percent that of hydrogen, making it the second most abundant element. In HII regions it is found mainly as singly ionized helium He^+. The abundances of the next most abundant elements are so low

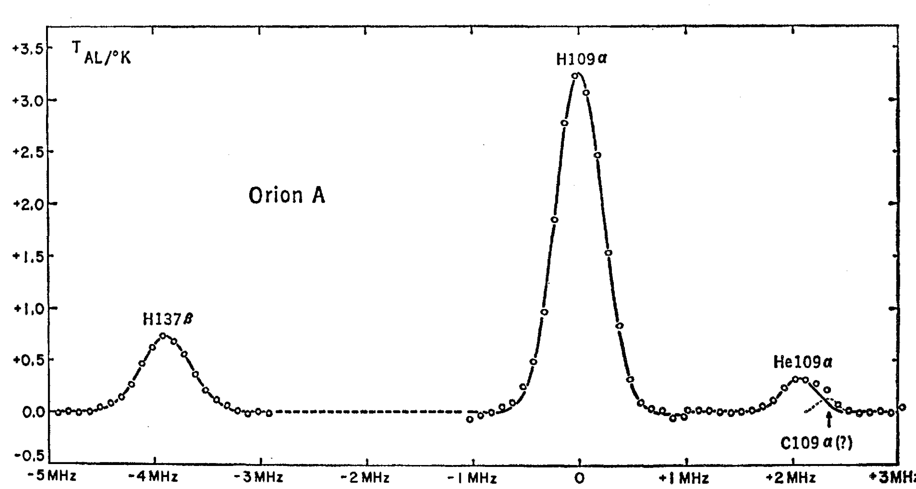

Fig. 2. The radio recombination line spectrum in the vicinity of the H109α-line (rest frequency of this line is 5008.9 megahertz) observed in the center of the Orion nebula. (Since the multichannel radiometer used for these observations was not wide enough, the lines had to be observed one after the other.) T_{AL} is the observed line antenna temperature.

that they were not expected to produce observable lines, but as described below, a process that may greatly enhance some of these lines has been suggested.

Table 2 gives Rydberg constants for some of the most abundant elements in interstellar space, and the frequencies of their 109α-recombination lines. The frequency of a line from an emitter of infinite mass is also given; therefore, 109α-lines from all elements fall within the 2.721-megahertz interval. A numerical evaluation of Eq. 1 for various elements and transitions is given by Lilley and Palmer (*11*).

Observations of the Radio Radiation from HII Regions

Observations of the free-free continuum radiation of HII regions have been made since the early days of radio astronomy. Most galactic HII regions are observed against a "hot background" caused by relativistic electrons (that is, electrons with velocities close to that of light) that are deflected in the magnetic field of the galaxy and thus radiate energy, known as synchrotron radiation (or magneto-bremsstrahlung). The spectrum of galactic synchrotron radiation, that is, the flux density S_ν as a function of frequency, decreases rapidly with frequency, from $S_{\text{synch}} \propto \nu^{-0.5}$ at meter wavelengths to $S_{\text{synch}} \propto \nu^{-0.9}$ at centimeter wavelengths. On the other hand, the spectrum of free-free radiation increases with the square of the frequency and then stays approximately constant (Fig. 1a). For this reason, plus the fact that radio telescopes have better angular resolution at shorter wavelengths, continuum observations of HII regions are preferably made in the centimeter wavelength range.

The possibility of observing recombination lines in the radio region was first suggested in 1959 by Kardashev (*8*). It subsequently took about 6 years and what is, at the moment, the most powerful radio telescope at centimeter wavelengths to yield an unambiguous detection of one of the hydrogen recombination lines. Marginal or qualitative results only had previously been obtained by several observing groups in Russia and by observers using the National Radio Astronomy Observatory (NRAO) 85-foot (26-meter) telescope. [A summary of earlier recombination line observations is given in (*12*).] On 9 July 1965, using a parametric amplifier radiometer with the NRAO 140-foot telescope, Höglund and Mezger detected the $H109\alpha$-line in Orion A and M 17 (*12*). The signal-to-noise ratio of the observed line profiles was good enough to allow a quantitative discussion of the results, and two surprising facts were found: (i) electron temperatures derived from the ratio of the observed temperature of the line to that of the continuum were much lower than electron temperatures derived from optical observations, and (ii) the shape of the line could be well approximated by a Gaussian curve. The shape of a line profile depends on a number of factors. Thermal and turbulent random motions of the emitting atoms produce a Gaussian-shaped profile by means of the Doppler effect, while interactions of the bound electrons with nearby free charged particles cause pressure broadening (sometimes also referred to as Stark broadening), which yields profiles with much broader wings. When the formulas that describe the pressure broadening in optical lines were extrapolated to radio frequencies, the radio recombination lines were expected to be completely washed out. This seems to be one of the principal reasons that radio astronomers did not search for these lines earlier.

Although the system noise of the line radiometer used for the first detection of the $H109\alpha$-line was relatively high, the NRAO observers extended their line and continuum survey to about 20 galactic sources (*13, 14*). The combination of these and other radio observations yields the distances and physical parameters of the investigated HII regions, as will be shown in the following section.

It took the Harvard observing group only a few weeks to tune their OH-line radiometer to the frequencies of the adjacent hydrogen recombination lines and to confirm the NRAO observations (*15*). The analysis of the Harvard observations agreed with that of the NRAO observations: low electron temperatures and no pressure broadening of the line profiles. In fact, the observed line widths in M 17 for the 109α-, 156α-, 158α-, and 166α-lines were directly proportional to the line frequencies, which again implies that only Doppler broadening is present (*7*). This result is particularly striking because an electron in the levels emitting the radio lines is very weakly bound to its nucleus and would appear to be subject to all kinds of perturbations by the surrounding charged particles.

In an attempt to observe enhanced emission of recombination lines, suggested by the work of Goldberg (*16*) (to be described below), and to test a pressure-broadening theory developed by Griem (*17*), the Harvard observers searched for the $H253\alpha$-line at 404 megahertz. The line was detected in the North American Nebula (*18*), and the results agreed with those obtained at higher frequencies: The electron temperature computed from Kardashev's formula was lower than that determined optically and, as predicted by Griem, no pressure broadening was observed. It is of interest to note that the 253α-line comes from the largest atom ever observed spectroscopically. The radius of the orbit of the electron when n equals 253 is about 3 microns.

At present, observing groups in the United States, Russia, and Australia are working on, or have completed, various programs for the observation of recombination lines. Some of their results will be mentioned in the following sections. In the winter of 1967 a considerably improved line and continuum radiometer for the frequency band surrounding the $H109\alpha$-line ($\nu_L = 5009$ Mhertz) was installed on the NRAO 140-foot telescope and was used by observers from Harvard, MIT, and NRAO for a variety of programs for the observation of recombination lines and the continuum. This observing period was the first time that a closed-cycle refrigerator system was used to cool a parametric amplifier for actual radio astronomy observations. The performance of the radiometer was very satisfactory, yielding a system noise temperature of about 80°K with the telescope pointed toward the zenith. As an example of the sensitivity of the radiometer, a spectrogram of Orion A is shown in Fig. 2.

Interpretation of Observations

Measurements of the continuum and of recombination lines utilize different observing techniques and yield complementary information on the physics of an HII region. In this section we will look at the study of NGC 6357 as a typical example. The quantities observed and derived for it are collected into Table 3.

In observations of the continuum, the most usual technique is to scan a certain region of the sky at a fixed frequency and to record the antenna temperature as a function of the telescope position. From these data a contour map, such as that of NGC 6357 shown in Fig. 3 superposed on an optical photograph of the region, can be constructed. This gives the equivalent of an optical photograph, although details are smeared because of the angular resolution of the telescope. The angular resolution depends on the size of the telescope beam (which was 6 minutes of arc at 6 centimeters for NGC 6357 when it was observed with the NRAO 140-foot telescope) and details of size $d < \theta D$ (where θ is angular resolution and D, distance to source) will not be resolved; in the case of NGC 6357, D = 1 kiloparsec (or 10^3 parsecs) and so d = 1.7 parsecs. Hence parameters found from observation are average values over a large volume of the HII region.

There is very little similarity between the optical photograph and the radio contour map. The only nebulosity visible in this photograph is the small patch below the rightmost source. The optical telescope has an angular resolution of 1 second of arc. However, the great difference between the two pictures is not due to the great difference in angular resolution, but to the absorption and scattering of light from the nebula by intervening dust. The area of apparent low density of stars running across the nebula and into the lower right-hand corner is due to this obscuration by dust. This photograph clearly demonstrates the importance of making radio observations of HII regions.

Observations of the continuum give positions and sizes of sources, and the brightness temperature and flux density at a particular frequency. The map of NGC 6357 shows three distinct components that are named according to their galactic coordinates (*13*). The observed quantities of these emission centers are listed in Table 3 with peak temperature T_C, the angular diameter θ_C and the flux density S_ν in lines 1, 2, and 3. When measurements at several frequencies are made, a continuum spectrum can be deduced, which yields information on the physics of individual HII regions and on the details of the region unresolved by the telescope.

For observations of radio recombination lines the receiver is made to switch between two frequency bands, one containing the line and the other adjacent to it. (In some cases load-switching is used rather than frequency-switching.) These bands are subdivided into a number (for example, 20 or 50) of individual channels. To make a measurement, the telescope is pointed at the source and the antenna temperature in each frequency band is compared, channel by channel, to obtain the excess line temperature (Fig. 2).

The observed line profile gives us the parameters already mentioned, that is, the peak temperature, T_L, of the line and its half-power width, $\Delta\nu_L$, (lines 4 and 5 of Table 3), and the difference between the center frequency and the rest frequency of the line, the so-called Doppler shift.

Substitution of T_C, T_L, and $\Delta\nu_L$ in a relation similar to that given in Eq. 2

Table 3. Physical conditions in NGC 6357, derived from continuum and recombination line observations at 5 gigahertz; fu, flux units (1 fu $\cong 10^{-26}$ watt m^{-2} $hertz^{-1}$).

Measurements	Component G353.2+0.9	Component G353.2+0.7	Component G353.1+0.4
	Observed quantities, radio continuum		
1. T_C/°K	16.0	14.9	3.9
2. $\frac{\theta_C = (\theta_\alpha\theta_\delta)^{1/2}}{\text{minute of arc}}$	8.2	10.9	9.6
3. S_ν/fu	156	215	47
	Observed quantities, radio line		
4. T_L/°K	0.83	0.84	0.20
5. $\Delta\nu_L$/khz	575	493	453
6. $\frac{V_r(\text{LSR})}{\text{km/sec}}$	−5.2	−3.7	−6.4
	Derived quantities, radio line		
7. T_e/°K	4800	4220	5660
8. $\frac{\langle V_t \rangle_{rms}}{\text{km/sec}}$	23	19	16
	Derived quantities, optical		
9. D/kparsec	1.0	1.0	1.0
	Derived quantities, radio continuum		
10. N_e/cm^{-3}	250	187	111
11. $M/M_\odot$	140	245	100
12. R_s/parsec	1.76	2.33	2.05
13. $\frac{u}{\text{parsec} \times cm^{-2}}$	69.8	76.2	47.3
14. $\frac{E}{\text{parsec} \times cm^{-6}}$	2.2×10^5	1.6×10^5	5.1×10^4

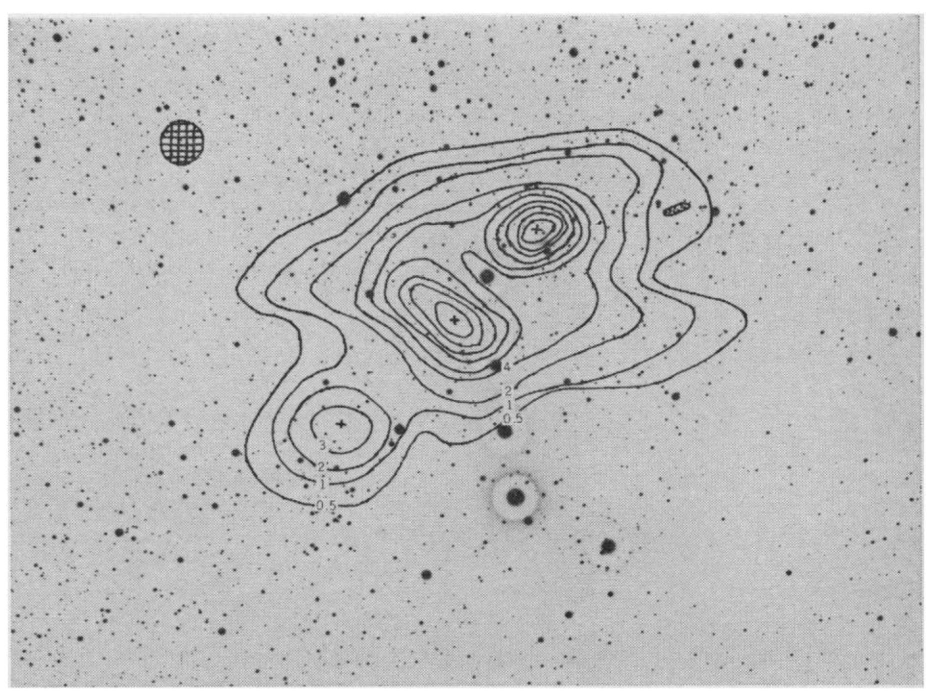

Fig. 3. Radio contours of the HII region NGC 6357 superposed on a (negative) photograph. The radio contours are lines of constant surface brightness (given in antenna temperature in degrees Kelvin). The unlabeled contours increase in steps of 2°K from the labeled ones. Crosses indicate the positions of the sources listed in Table 3. Black spots surrounded by circles are stars in the foreground that are unrelated to the nebula. The brightest of these is a 6th-magnitude star, too faint to be seen with the unaided eye.

yields the electron temperatures given in the seventh line of Table 3. The thermal motion of the hydrogen atoms alone cannot account for the observed widths of the H109α-lines. This indicates that in addition to the thermal motion there is turbulent motion in the HII region. The root-mean-square velocity $<V_t>_{rms}$ of this turbulent motion inferred from the line widths is given in line 8. In NGC 6357 and in most other galactic HII regions, the root-mean-square velocity of turbulent motions turns out to be supersonic (*14*).

The radial velocity, V_r, that is, velocity of the source along the line of sight, can be calculated from the observed Doppler shift from the formula $V_r = -(\Delta\nu/\nu_L) \times c$, where c is the velocity of light. The radial velocity includes effects due to the rotation of the earth, its revolution about the sun, and the peculiar motion of the sun with respect to the average motion of nearby stars. When these are subtracted, a velocity with respect to the average motion of our part of the galaxy is obtained—the so-called velocity with respect to the local standard of rest, V_r(LSR). This quantity is useful in studies of the large-scale structure of the galaxy. For the components of NGC 6357 the radial velocities are given in line 6 of Table 3.

The galaxy is known to be rotating. The sun will make one complete revolution about the galactic center in 1 "galactic year" (about 200 million years). The velocities of HII regions are caused by galactic rotation and individual peculiar motions. However, the galaxy does not rotate as a rigid body, but the rate of rotation depends on the distance from the center of the galaxy. Determining this law of variation of rotational velocity is one of the interesting astrophysical problems that can be studied by observations of recombination lines but, conversely, knowing the rotation law we can determine the distance of an HII region from its radial velocity (the so-called kinematic distance). It should be kept in mind, however, that there are large deviations from circular orbits in at least some parts of our galaxy. Thus kinematic distances are at present rough estimates of the possible distance range of galactic objects. For HII regions whose distances from the galactic center are less than the distance of the sun from the center (10 kparsec), there are two kinematic distances compatible with a given radial velocity. This ambiguity problem arises for most of the distant HII regions. Methods of deriving kinematic distances and resolving this distance ambiguity and the errors involved are discussed by Mezger and Höglund (*14*) and by Dieter (*19*). These methods provide a powerful tool for research on galaxies, especially if the distances of the HII region are so large ($D > 2$ kparsec) that optical methods fail to work. In the case of the nearby HII region NGC 6357 the distances of all three components, as given in the ninth line of Table 3, are based mainly on optical observations.

At a frequency of 5 gigahertz, most HII regions are optically thin, so that their surface brightness is proportional to the emission measure, which is the integral of the square of electron density taken along the line of sight s.

$$E = \int_{s_1}^{s_2} N_e^2 \, ds \qquad (3)$$

In this integral the line of sight is given in parsecs and the electron density per cubic centimeters, so that the dimension of the emission measure becomes parsecs $\times$ centimeters^{-6}. Values of the emission measures of the bright emission centers of NGC 6357 are given in line 14 of Table 3.

Thus, from the measurements of the continuum flux and knowing the distance to the HII region, we are able to get at the density and the total mass. In order to determine these quantities, however, we must assume a model of the HII region. Details of the method and comparisons between various models are given by Mezger and Henderson (*13*), but for our present purpose we will merely state that for most reasonable models the density and total mass derived are quite similar. We have assumed that the emission centers are spherical and have uniform density and temperature to obtain the values given in lines 11 and 12. From the radius and density, the excitation parameters $u = R_s N_e^{\frac{2}{3}}$ are computed (line 13), which are directly related to the Lyman continuum flux of the exciting star. The numerical value of u is equal to the Strömgren radius for a density $N_e = 1$ cm^{-3}. Comparison with column 6a of Table 1 shows that stars of spectral types O4 through O6 are needed to account for the ionization of the bright emission centers in NGC 6357. This example shows that from radio observations the distance and the physical parameters of an HII region can be determined and that it is even possible to estimate the spectral type of the exciting star. Thus HII regions can be studied even if they are located at the opposite side of the galactic center. Only the angular resolution and the sensitivity of our radiometers now set a limitation to the radio exploration of our galactic system.

Physics of the Emission of Radio Recombination Lines

Two interesting physical problems were raised by the work of the NRAO and the Harvard observers: the absence of pressure broadening in the radio recombination lines and the apparent low electron temperatures derived from these lines. The first of these two problems to be solved was the absence of pressure broadening. The equations used by Kardashev (*8*), which were an extrapolation of results obtained for optical lines, were simply inapplicable at the low densities of HII regions and the large principal quantum numbers involved in the emission of radio recombination lines. The idea that because the electron is quite distant from the nucleus it should be perturbed strongly is correct, but the apparently obvious conclusion that the line will therefore be considerably broadened is incorrect, because most collisions disturb both the upper and the lower energy levels in the same way so that the difference between them remains the same. These facts were first demonstrated by Griem (*17*), who computed broadening of the line rigorously and found that the amount of broadening to be expected for any of the lines so far observed would be concealed by the observational noise.

When observations are carried out with high signal-to-noise ratios at low frequencies, the pressure broadening should be measured and the electron density in the region from which the line is emitted can be determined. If the density fluctuations are large within HII regions, this density may be much greater than the average density determined by the observations at the radio continuum.

Because the electron temperatures determined from the $n\alpha$-lines were so different from those previously believed to prevail in HII regions, Goldberg (*16*) reexamined the derivation of the equation used to calculate electron temperatures from observations of recombination lines. He found that the error could be in the assumption that the energy levels of hydrogen in HII regions are populated as they would be in thermodynamic equilibrium. Actually, physical conditions in HII regions are very different from those of thermodynamic equilibrium. The atoms and ions are exposed to the strong anisotropic radiation field of the exciting star, there are macroscopic mass motions, the density varies from point to point, and the populations of energy levels responsible for optical lines are far from the values of thermodynamic equilibrium. In fact, it may appear surprising that considerations of thermodynamic equilibrium make sense at all. However, the free electrons in the ionized gas interact so strongly and rapidly with the surrounding charged particles that they quickly come to equilibrium so that in any small (but macroscopic) region they have a well-defined temperature. Because of this it is very convenient to relate all other physical processes to the temperature of the free electrons, the so-called electron temperature. The actual number of atoms in the level with principal quantum number n is given by the population of this energy level, in the case of thermodynamic equilibrium, multiplied by a factor b_n which depends on both electron temperature and electron density. Thus the b_n factor describes a deviation from thermodynamic equilibrium. (In the remainder of this article we will use the phrase "thermodynamic equilibrium" to mean only that the energy levels are populated as they would be in thermodynamic equilibrium at the temperature of the free electrons, that is, $b_n = 1$.) Theoretical study of the recombination process in gaseous nebulas (often referred to as the theory of statistical equilibrium) was begun in the 1930's and the calculations of the b_n factors for hydrogen for the values of n that were of interest to optical spectroscopists were carried out. For small values of n, b_n can be much different from unity; but for larger values of n, b_n increases slowly with n and approaches unity as n approaches infinity. Calculations by Seaton (*20*) showed that b_n differed from unity by only a few percent for the values of n involved in the radio lines. Goldberg pointed out that while b_n was very nearly unity, the increase in b_n from one level to the next was sufficient to make each level overpopulated with respect to the level below it and thus lead to a maser-like enhancement of the line. He solved the equation of transfer, taking this effect into account, but we will quote the result for small optical depths only:

$$\frac{T_L}{T_C} = \left(\frac{T_L}{T_C}\right)_{TE} b_n \left[1 + \frac{\tau_C}{2}\frac{kT_e}{h\nu}\left(\frac{b_n - b_{n'}}{b_n}\right)\right] \qquad (4)$$

where (T_L/T_C) is the observed ratio, $(T_L/T_C)_{TE}$ is the ratio that would obtain in thermodynamic equilibrium, and the subscripts n and n' refer respectively to the upper and lower energy levels involved in the transition. In this equation, τ_C is the optical depth of the radio continuum; k, the Boltzmann constant; and h, the Planck constant. Comparison with Eq. 2 shows that if the line is enhanced, the electron temperature computed from Eq. 2 will be too small. Since $kT_e/h\nu$ is so large at radio frequencies (of the order of 10^5 for typical temperatures and frequencies), $(b_n - b_{n'})$ need only be of the order of 10^{-5} to have significant effects. Note that this is in contrast to most maser and laser applications in which very large overpopulations are obtained.

Using values of b_n computed by Seaton, Goldberg found that the lines would be enhanced by about the right amount to bring the determinations of optical and radio line temperatures into agreement. Because the radio lines provide a means to study directly the behavior of b_n for large values of n, interest has increased in the relatively old subject of statistical equilibrium in gaseous nebulas. Recently, calculations of the b_n factors have been carried out at several institutions in order to improve upon Seaton's original approximate calculation (*21*). Since, however, the b_n factors depend on both electron density and temperature whose variations are usually not very accurately known, a direct comparison between theory and observation is rather difficult.

The departures from thermodynamic equilibrium affect hydrogen line intensities only by relatively modest or negligible amounts. However, in the course of a program to observe helium 109α-lines, we found a more striking example of departures from thermodynamic equilibrium when we

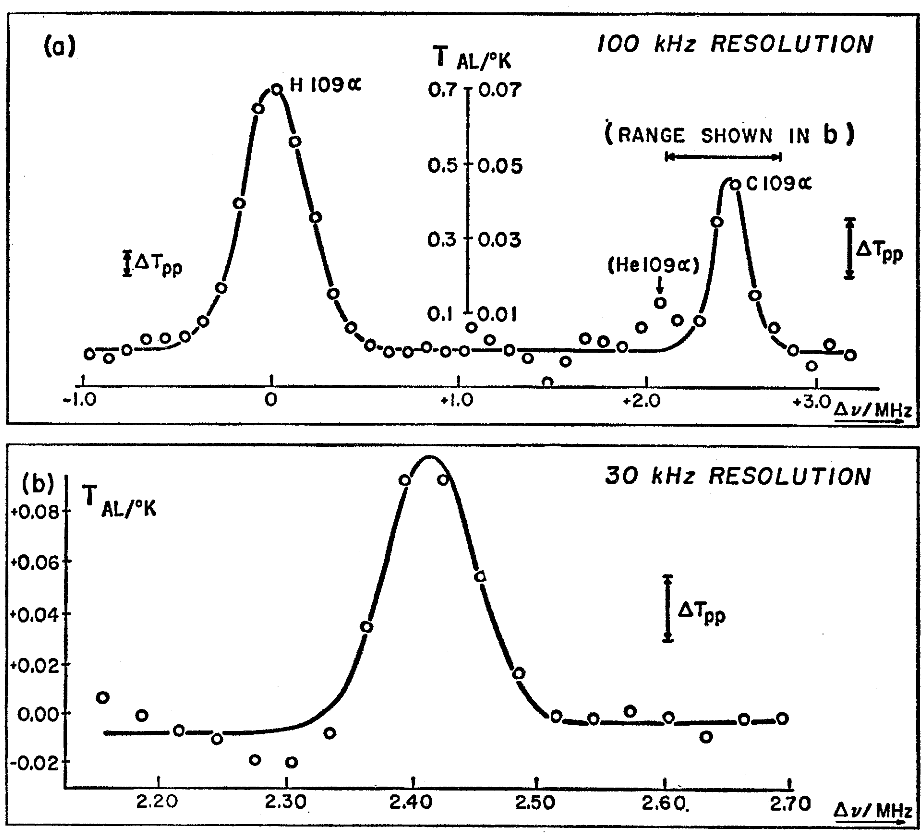

Fig. 4. (a) The radio recombination line spectrum of NGC 2024, including the H109α- and the He109α-lines. The helium signal is not significantly larger than the noise, but inadvertently a new line that was later identified as a recombination line of the carbon (C) atom (*22*), was detected during this observation. (b) The C109α-line shown in (a) is observed here with a higher frequency resolution. ΔT_{pp} is the peak-to-peak noise fluctuation in the observation.

Table 4. Ratio of the intensity of He109α to that of H109α. Italic numbers in parentheses are references.

Source	N(He)/N(H) from He109α and H109α-line observations	N(He)/N(H) from previous studies
M 17	0.090 ± 0.010	0.10 ± 0.05 (*25*)
Orion	.077 ± .010	.143 ± .02 (*26*)
NGC 6357	.09 ± .02	
IC 1795	.09 ± .02	
W 51	.09 ± .02	
NGC 2024	< .02	

unexpectedly detected the recombination line from another element (*22*). In thermodynamic equilibrium, the intensity ratio of α-lines from different elements would simply be the abundance ratio, and since the most abundant elements after hydrogen and helium have abundances of the order of only 10^{-3} to 10^{-4} of hydrogen, their radio recombination lines would be too weak to detect. The observed spectrum of NGC 2024 is shown in Fig. 4. No significant helium signal is observed, but a narrow line, unresolved with the 100-kilohertz resolution, is seen at a higher frequency than the expected position of the He109α-line. Observations carried out at the predicted frequency of the 110α-line demonstrated that this was indeed a recombination line. Reasons why this new line is not a hydrogen or helium recombination line are discussed by Palmer *et al.* (*22*), but the principal reason is that the line-width is so narrow that it must come from an emitter of mass ≥ 12 times the mass of hydrogen. The width corresponds to a maximum temperature of 750°K for hydrogen and 3000°K for helium. Anomalous lines were also detected in IC 1795, Orion, and W 51. The frequency shifts from hydrogen were found to be different in each case, showing that if they are lines from the same emitter, that emitter cannot be directly identified on the basis of rest frequency. Therefore, the identification must be made less directly by theoretical reasoning.

Goldberg and Dupree (*23*) have interpreted these lines as α-lines of neutral carbon. This requires a line enhancement of at least 60, which in turn requires large departures from thermodynamic equilibrium. They have shown that very large departures from thermodynamic equilibrium may obtain for complex atoms and ions in the physical conditions found in HII regions because the levels may be predominantly populated by dielectronic recombination. (In this process an electron is recaptured through an intermediate, doubly excited state.) Since this process favors levels with large n, very large populations can result for these levels. Goldberg and Dupree have calculated that, for calcium, values of b_n may exceed 1000. The abundances, the dielectronic recombination rates at the temperatures of HII regions, and ionization potentials for various elements all suggest that carbon is the most likely candidate (*23*). The process of dielectronic recombination had never before been considered for HII regions. Thus these observations make it necessary to completely reexamine the theory of statistical equilibrium of HII regions for ions that can recombine by dielectronic recombination; and they also point to the possibility of observing many more elements than previously expected if regions are found with appropriate physical conditions.

We mentioned before that the frequencies of the radio recombination lines of other atoms are expected to differ from those of hydrogen only by the reduced mass factor in the Rydberg constant (Table 2). It was an obvious choice, therefore, to use radio recombination lines to study the relative abundance of helium to hydrogen in HII regions. Such measurements are difficult to make in the optical region. First, the optical spectra of HII regions are difficult to observe for the same reason that it is relatively easy to observe HII regions with radio techniques: The objects are very extended so that in general little of their emission is collected by an optical telescope, while they emit over a relatively large fraction of the radio telescope beam. Second, the optical measurements must be corrected for interstellar reddening. The abundance determination by radio observations is made by comparing the total energy emitted in an H$n\alpha$- and an He$n\alpha$-line with the same principal quantum number n. We then obtain a ratio of the weighted average of the number of singly ionized helium ions to a weighted average of the number of protons. If we assume that the effect of possible deviations from thermodynamic equilibrium are the same for the two lines and that the spatial distribution of hydrogen and helium ions are the same, the weightings are identical so that the ratio of the line intensities is equal to the abundance ratio. These assumptions are discussed in detail by Palmer *et al.* (*24*). The first observations of a helium recombination line were made in M17 (*25*); our recent observations are summarized in Table 4. The observed values of the line intensity ratio are shown in column 2. The values are distinctly lower than the value of 0.143 determined from the optical spectrum of Orion (*26*), but nearer to values inferred from the theory of stellar evolution for young galactic objects (*27*). The explanation for this difference is not yet known but may be due either to a failure of one of the above assumptions or to an error in the optical determinations caused by uncertainty in the reddening correction.

Electron Temperature of HII Regions

An HII region is heated by ionization of the plasma by starlight and is cooled by radiation, mainly by forbidden optical and infrared lines of the oxygen, neon, and nitrogen present, since the most abundant elements are rather inefficient radiators. Therefore, the electron temperature depends (weakly) on the surface temperature of the star, which determines the energy distribution of the ionizing photons, and (strongly) on the composition of the gas, which determines the cooling rate of the plasma. It is interesting to note that without the "trace elements," such as oxygen, neon, and nitrogen, the electron temperatures would be 50,000° to 100,000°K, about a factor of 10 greater than any actually observed.

As mentioned in the preceding section, the electron temperature is the basic quantity defining the physical

Table 5. Electron temperatures of some HII regions obtained by different methods. Italic numbers in parentheses are references.

Source	$\frac{\Delta\nu_L T_L\ (\mathrm{H}109\alpha)}{\Delta\nu_L T_L\ (\mathrm{H}137\beta)}$	$(T_e)\alpha$	$(T_e)\beta$	T_{optical} (*36*)	$T_{\mathrm{free\text{-}free}}$ (*32*)
Orion	5.39 ± 0.25	7100	9700	10,000	3000
NGC 2024	4.58 ± .35	7550	9150		4000
M 17	4.17 ± .50	6100	6450	8100	

state of an HII region. For example, the observed radio surface brightness temperature is directly related to the electron temperature. Consequently, all other parameters of an HII region, such as its total mass, density, and emission measure, which are derived from radio observations, depend on the adopted value of the electron temperature.

Electron temperatures are measured mainly by comparing two observable quantities, for instance, two spectral lines or one line and the adjacent continuum, which depend on the electron temperature in different ways. Optical observations use mainly the ratio of two forbidden lines of doubly ionized oxygen, whereas the corresponding radio method uses the ratio of a hydrogen recombination line to the adjacent free-free continuum (see discussion above or Eq. 2).

Optically determined values of electron temperatures of galactic HII regions range from 6000° to 10,000°K, whereas the evaluation of H109α- and H158α-line observations, by means of Eq. 2, of a considerably larger number of galactic HII regions yields temperature values between 3000° and 9000°K (*14, 19*). Electron temperatures, as derived optically, in some cases exceed the corresponding value derived from radio recombination lines by as much as 3000°K. The main criticism of the radio method is that the effect of deviations from thermodynamic equilibrium in the radio line emission is not known. If, for example, the radio line radiation of an HII region were enhanced by a factor 2, its electron temperature derived from Eq. 2 would be too low by a factor of $2^{-1/1.15} = 0.55$.

In order to determine the magnitude of the effects of departures from thermodynamic equilibrium, the most obvious thing to do is to observe α- and β-lines originating from the same level (*28*). This experiment has not been tried yet because of the lack of the necessary receivers. However, the 137β-line was observed together with the 109α-line (*29*). Earlier observations (*30*) of the 158β-line and 126α-line in Orion had indicated that the intensity ratio was not that expected in thermodynamic equilibrium, but the 158β-line was not observed with sufficient integration time to make the result conclusive.

The 137β-line was observed with high signal-to-noise ratio in Orion (see Fig. 2), M 17, and NGC 2024. The expected intensity ratio was 3.58, but the observed values, as shown in the second column of Table 5, were significantly different from this, thus showing that at least one of the energy levels responsible for the two compared cannot be

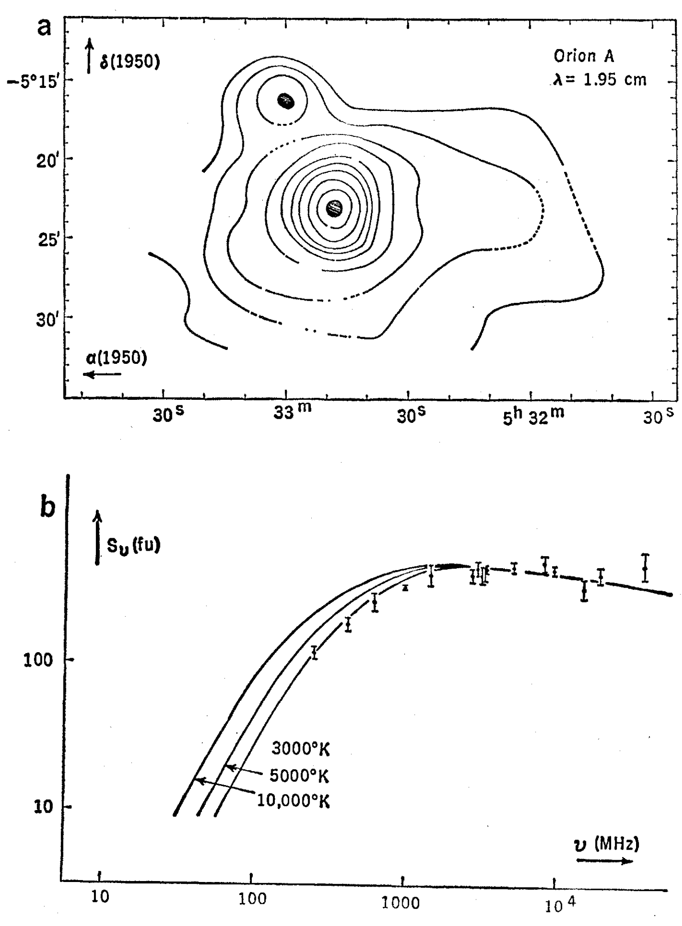

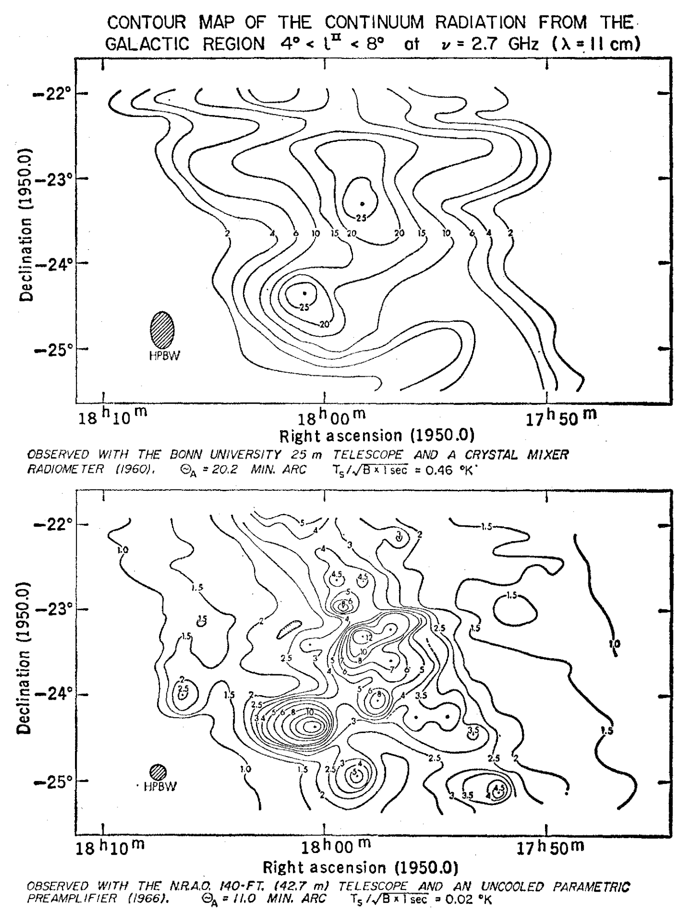

Fig. 5 (left). (a) Radio contour map of the Orion nebula. The intense emission center is known as NGC 1976 (M 42); the weaker emission center in the northern part of the nebula, as NGC 1982 (M 43). Angular resolution of the observations is 2 minutes of arc (*32*). (b) Based on the contour map in (a), the low-frequency continuum spectrum of the Orion nebula was computed for different electron temperatures. Comparison with observations yield an electron temperature of about 3000°K (*32*). Fig. 6 (right). Two contour maps of the same region of the galaxy (at galactic longitudes $l^{II} \simeq 6°$ and in the vicinity of the galactic plane) observed at the same wavelength (11 centimeters) but with different radio telescopes and radiometers. The difference in the quality of the two contour maps demonstrates the enormous improvement in radio astronomical observations during the past few years due to the construction of large radio telescopes and the invention of low-noise radiometers, such as parametric amplifiers (*44*). The hatched area labeled *HPBW* is the angular resolution of the radio telescope (θ_A). The quality factor $T_S/(B \times 1 \text{ sec})^{\frac{1}{2}}$ is the theoretical root-mean-square noise expected for 1-second integration time. T_S is system noise temperature; *B*, the bandwidth.

populated according to thermodynamic equilibrium. The third and fourth columns of Table 5 give the electron temperatures derived from the observed H109α- and H137β-lines, respectively. The corresponding electron temperatures, as derived from optical observations, are given in column 5. There is obviously a better agreement between optical and H137β temperatures. A similar result has been obtained by comparing the 94α- and 148δ-lines in Orion (*31*). This observation has the added interest that the 148δ-line is the highest-order (largest value of Δn) radio line so far observed.

There are obviously departures from thermodynamic equilibrium in the observed ratios of the α-lines to their adjacent higher-order transition lines (that is, β-lines with $\Delta n = 2$, γ-lines with $\Delta n = 3$, and so on). However, arguments have been presented (*32*) that the electron temperatures derived from α-lines on the assumption of thermodynamic equilibrium are in fact close to the true average electron temperature of HII regions. This implies that the present theory of the radio recombination spectra is not correct.

The analysis of the free-free continuum spectrum of an HII region provides another and independent means of determining the electron temperature from radio observations. The basis of this method is that if we know the distribution of surface brightness of an HII region (as shown in the contour map of the Orion nebula, Fig. 5a) at a frequency at which the HII region is optically thin, we can predict the flux at any other frequency as a function of the electron temperature. The solid points in Fig. 5b show the observed free-free continuum spectrum of Orion A. The full curves are the computed spectra for different values of the electron temperature. The curve that best fits the observations corresponds to an electron temperature of about 3000°K (*32*). A similar analysis of the continuum spectrum of NGC 2024 yields an electron temperature of 4000°K (last column of Table 5). These values are even lower than the H109α temperatures.

Earlier theoretical estimates of electron temperatures of HII regions yielded values of 10,000°K. However, more recent computations (*33*) showed that temperatures between 4000° and 7000°K are more likely.

Summarizing the observational results, one finds that optical observations usually yield the highest and radio continuum observations the lowest electron temperatures. How can these different electron temperatures be reconciled? The answer may come from the fact that electron temperature is a local property: It is defined only for small regions so that a priori we have no reason to expect that the whole HII region will have the same temperature. Computations by Hjellming (*34*) and Rubin (*35*) have shown that the electron temperature may vary by several thousand degrees within an HII region. All observations yield some kind of weighted average electron temperature, but the weighting is different for different meth-

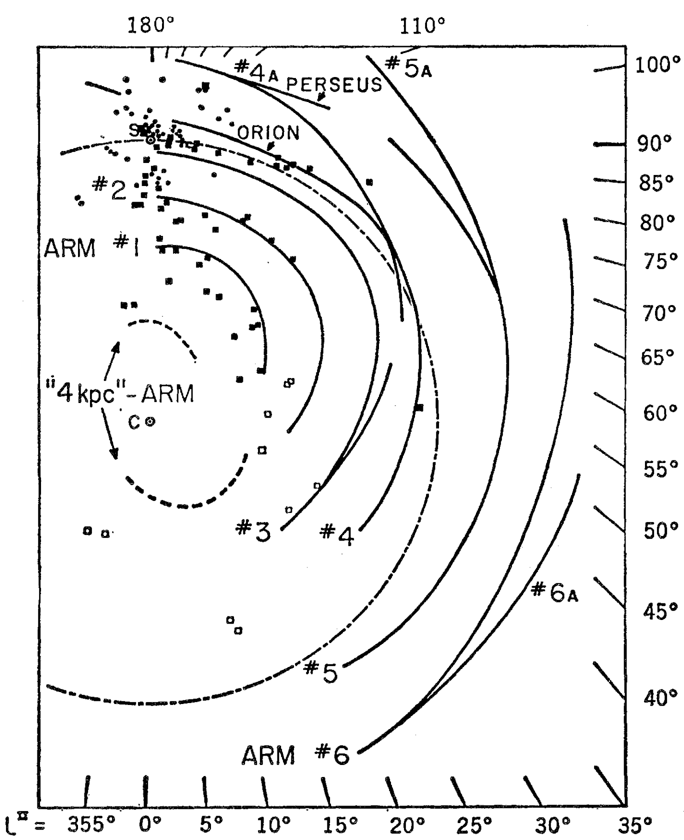

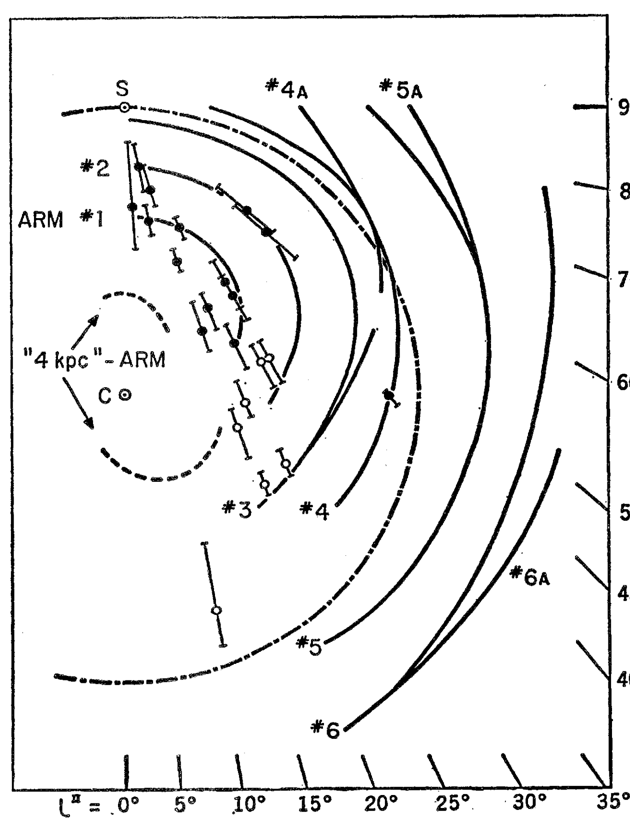

Fig. 7 (left). Distribution of neutral hydrogen (full curves) and HII regions (dots and squares) in the northern part of the galactic plane. The curves indicate the location of density maxima in the neutral hydrogen (*41*). Dots represent HII regions whose distances have been determined optically (*40*), and squares represent HII regions whose distances have been determined from the Doppler shift in their H109α-line (*37*). In some cases two kinematic distances are compatible with observations; then the farther distance is also indicated by an open square. The names *Orion* and *Perseus* refer to the designated arms. The sun and the galactic center are labeled *S* and *C*, respectively. Fig. 8 (right). Distribution of neutral hydrogen and giant HII regions in the northern part of the galactic plane. These giant HII regions are probably clusters of very young O and B stars. Error bars in the position are due to peculiar motions of the HII region that may be superposed on the galactic rotation. In cases where two kinematic distances are compatible with observations the farther distances are also indicated by open circles (*37*). *S*, sun; *C*, galactic center.

ods. This has been discussed in detail by Peimbert (*36*). The optical methods favor regions of high, and the radio methods regions of low electron temperatures. The analysis of the free-free continuum spectrum yields the electron temperature in the outer parts of an HII region (*32*), which seems to be considerably lower than the electron temperature close to the exciting star. Such an effect is predicted by theoretical investigations (*34, 35*), because in the dense central part of an HII region the cooling by forbidden-line radiation becomes less efficient because of collisional de-excitation of the metastable energy levels that radiate the forbidden lines.

Large-Scale Structure of Our Galaxy

It is well known from optical observations that O and B stars and their associated HII regions define the spiral structure of external galaxies. Hence the determination of the positions and distances of the HII regions in our own galaxy would be expected to show its spiral structure. However, optical observations of HII regions in our galaxy are restricted to the relatively small region within 2 or 3 kiloparsecs from the sun by heavy absorption of light by interstellar material. (Our galaxy has a diameter of approximately 30 kiloparsecs.) Radio waves, on the other hand, propagate through interstellar space with very little attenuation, so that the radio radiation of even the most distant HII regions can be detected. This has been known for some years, but only with the detection of radio recombination lines have radio astronomers had a tool with which to determine the (kinematic) distances of HII regions—the Doppler shift of the lines emitted. This technique for studying the large-scale distribution of galactic HII regions was applied by Mezger and Höglund (*14*) and later by Dieter (*19*). Subsequently a joint NRAO-MIT observing team (*37*) decided to undertake an extended survey of the H109α-line of all detectable galactic sources. At that time only a very limited number of galactic radio sources were known from previous continuum surveys with 25-meter telescopes at 21.5- (*38*) and 11-centimeter (*39*) wavelengths. In the meantime both larger radio telescopes and more sensitive radiometers became available, and it was clear that the H109α-line survey had to be preceded by a complete survey of the continuum radiation of the part of the galaxy that is visible from Green Bank, West Virginia, the site of the NRAO.

To illustrate the improvement in results, Fig. 6 shows previous and present maps of an area of the galactic plane—this is a good demonstration of the enormous progress in radio astronomical instrumentation during the past few years.

During the first phase of the NRAO-MIT observing program, the H109α-line emission of 80 sources was surveyed and the line was found in 52 sources. In Fig. 7 the positions of these HII regions projected on the galactic plane are plotted (filled squares). In cases in which the distance ambiguity could not be resolved the farther of the two possible distances is also plotted as an open square in the diagram. The dots represent HII regions in the vicinity of the sun, whose distances have been determined by optical observations (*40*). The full curves are spiral arms as outlined by recent 21-centimeter observations by Henderson (*41*), that is, these curves represent the maxima in the distribution of the interstellar neutral hydrogen. We find a reasonable agreement between the location of HII regions and the dense clouds of neutral interstellar hydrogen (HI), the agreement becoming even better if the radial velocities of HII and HI are directly compared (*19*).

Figure 8 shows the distribution of what we can call "giant HII regions" —those requiring at least ten main-sequence O5 stars to account for their ionization; they are probably, as recent observations indicate (*3*), clusters of relatively young O and B stars. This distribution differs drastically from that in Fig. 7. In some cases the distance ambiguity could not be resolved, and then the farther distance is also shown as an open circle. All the giant HII regions (with two exceptions, W 49 and W 51) are found within galactic latitudes $0° \leq l^{II} \leq 30°$, and there is a distinct accumulation in a relatively narrow sector between 20° and 30° galactic longitude. Those giant HII regions that are obviously inside the 4-kiloparsec arm and close to the galactic center are not shown in the diagram, as their actual position is very uncertain.

The physical conditions just outside the 4-kiloparsec arm seem to be particularly favorable for the formation of O and B stars. The reason for this is still not clear, but the tentative explanation that Westerhout gave in 1958 to explain his continuum observations (*38*) still has a high degree of probability. Observations of the 21-centimeter line show that the neutral hydrogen inside the 4-kiloparsec arm is rapidly streaming outward from the center of the galaxy with velocities up to 200 kilometers per second. At a distance of about 4 kiloparsecs from the center this outward flow is braked, causing a concentration of neutral hydrogen that is seen as the 4-kiloparsec arm. This arm is still expanding outward with a velocity of about 50 kilometers per second, but at the same time takes part in the general galactic rotation. The first stages of star-formation will probably start in this region of high-density neutral hydrogen, but during the time it takes for the stars to contract to the main sequence they will have traveled farther outward. This could explain why most giant HII regions are located outside the 4-kiloparsec arm, that is, in a region where the density of neutral hydrogen is relatively low. In the other (outer) spiral arms, where galactic rotation dominates, HII regions are usually found close to the regions of highest density of neutral hydrogen.

HII Regions Associated with OH-Emission Clouds

The 18-centimeter lines emitted by the OH molecule were first detected as absorption lines. Later, and rather unexpectedly, these lines were found in emission, and their characteristics clearly showed that the emission mechanism of these OH lines must be a maser effect rather than thermal emission. It was also found that most of the OH-emission clouds are located close to HII regions, most of which are known as strong thermal radio sources (*1*). The close correlation between the radial velocities derived from the observed Doppler shifts of the OH lines and the radio recombination lines emitted by the associated HII regions showed that this coincidence in position was not an observational selection effect but that HII regions and OH-emission clouds are in fact closely associated in space (*42, 14*). Subsequently a program was started at the NRAO in which HII regions associated with OH-emission clouds were investigated. This program resulted in the detection of a new class of compact high-density HII regions that have possibly given a new insight

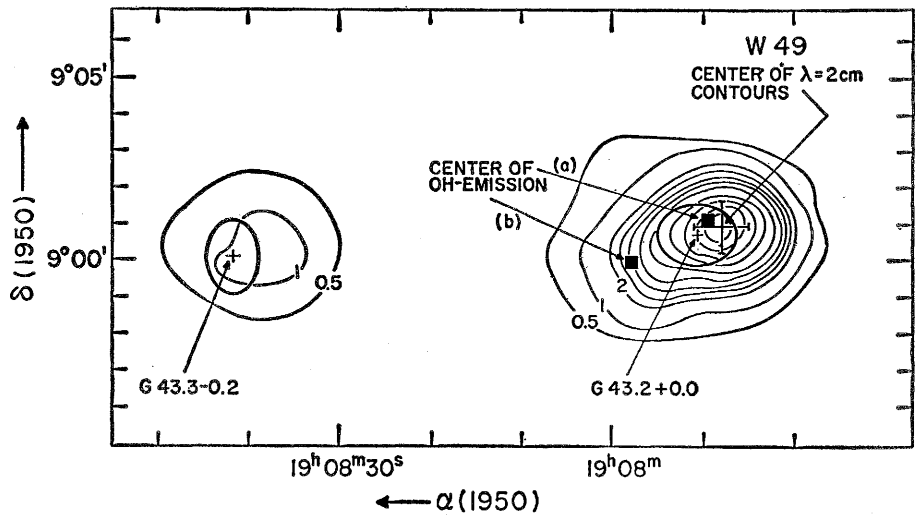

Fig. 9. Contour map of the radio source W 49, observed with an angular resolution of 2 minutes of arc. Component G43.3−0.2 (referred to in the text as component B) is a nonthermal source, probably a supernova remnant. Component G43.2+0.0 (referred to as component A) is an extended HII region, imbedded in which are high-density HII regions of very small angular diminsions (< 15 seconds of arc) and OH-emission clouds whose dimensions are smaller than 0.01 second of arc.

into the physical conditions of the formation of stars.

The first HII region to be studied in detail was W 49. It is located at a distance of 14.1 kiloparsecs from the sun and basically consists of a thermal component designated as component A and a nonthermal component B. The thermal component A is one of the giant HII regions shown in the diagram Fig. 8. The analysis of its free-free continuum spectrum showed that this HII region consists of a low-density HII region with an electron density of 234 per cubic centimeter, a total mass of $9.3 \times 10^3\ M_\odot$ and a diameter of 14.4 parsecs. Embedded in this low-density plasma are condensations with densities greater than 10^4 per cubic centimeter, containing altogether about 100 $M_\odot$ of ionized hydrogen. The total thermal component is surrounded by a relatively dense neutral hydrogen shell of mass up to $3.2 \times 10^5\ M_\odot$. The shell and HII system that might be an association of O and B stars in an early stage of evolution (*3*).

These compact HII regions may be the ionized shells of recently formed O stars. To account for the ionization of these condensations in W 49 between 6 and 11 O stars are needed. Evidence for a number of small high-density HII regions that may be associated with individual stars is provided by the fact that preliminary observations with the NRAO interferometer at a wavelength of 11 centimeters yielding an angular resolution of 20 seconds of arc, reveal complicated structure in distribution of the brightness temperature of the thermal component A (*3*).

A contour map made from observations at a wavelength of 2 centimeters, with an angular resolution of 2 minutes of arc (Fig. 9), shows that the high-density condensations are only partly resolved. The two OH-emission centers, shown in the map as filled squares, seem to be located inside the low-density HII region and close to the high-density condensations. The proximity of OH-emission centers and ionized shells of young O stars suggests a close correlation between the formation of stars and nonthermal OH emission.

W 49 is too far away to allow direct observations of one of the individual high-density HII regions; but similar compact HII regions were found to be associated with OH-emission sources in other, nearby HII regions. In IC 1795 (W 3), the source of OH emission is separated by about 14 minutes of arc from the center of radio emission. There was no conspicuous feature found to be associated with the OH source in either the optical range or the radio continuum. Only when observed at very short wavelengths is a weak point source, designated as G133.9 +1.1, found, the position of which seems to coincide with that of the OH-emission source. Another compact HII region, DR 21, was found in the Cygnus X region, and its H109α-line and its continuum emission over a wide band of frequencies were measured (*4*, *5*). Again, the associated OH-emission center is found to be close to the position of the compact HII region. The physical parameters of these compact HII regions are given in Table 6. They were obtained by fitting spherical model HII regions with uniform density to the observed continuum spectra.

In the case of the distant O- and B-star association W 49, we cannot determine the number n of compact HII regions directly, so models with $n = 6$ and $n = 11$ identical compact HII regions were assumed for our computations. A comparison of the excitation parameters given in the last of column of Table 1 with those in column 6a shows that even the weakest of these HII regions still requires an O7 star to account for its excitation. The sizes of these compact HII regions range from 0.06 to 0.4 parsec, their total mass of ionized hydrogen ranges from 0.6 to 15 solar masses.

The two nearby HII regions and their associated sources of OH emission reveal a pattern rather similar to that found in W 49, only on a much smaller scale. The compact HII regions appear as dense condensations with small dimensions that are embedded in an extended HII region of considerably lower density. The associated OH-emission sources seem to be located inside the low-density HII regions and close to the compact HII regions. How can we fit

Table 6. Physical parameters of some high-density HII regions associated with OH-emission sources.

Source	Distance (D/kparsec)	T_e/°K	E/parsec $\times$ cm^{-6}	Diameter ($2R_s$/parsec)	Density (N_e/cm^{-3})	Mass ($M_{HII}/M_\odot$)	Excitation parameter (u/parsec $\times$ cm^{-2})
$n = 6$				0.42	1.6×10^4	15.0	131
W 49; A 2	14.1	6000	1.0×10^8				
$n = 11$		(adopted)		0.31	1.8×10^4	7.2	107
DR 21	1.5–3	7600	2.0×10^7	0.22–0.44	$(9.5–6.7)10^3$	1.3–7.8	49–78
IC 1795	2.6	7000	5.7×10^7	0.06	3.0×10^4	0.6	30
G133.9+1.1		(adopted)					

these different pieces of information together? The suggestion by Davidson and Harwit (*6*)—that early-type stars at one stage of their evolution become "cocoon stars"—may well be correct. A cocoon star is a recently formed star that is still surrounded by the remnant of the originally contracting cloud out of which the star was formed. The ultraviolet radiation from the star transformed the inner shell of this remnant in an ionization-bounded HII region that must have characteristics similar to those given in Table 6. The outer part of the remnant forms the cocoon of dust and neutral matter that may be opaque to optical light. In fact Reddish (*43*) reports on optical observations that show that very young, early-type stars are surrounded by obscuring clouds having diameters ≤ 1 parsec and masses $\sim 30\ M_\odot$. The time needed for the formation of the initial Strömgren spheres of these high-density HII regions is short compared to the time it takes the star to evolve to a main-sequence star. Hence, a correct theory of the formation and evolution of these dense HII regions must consider the variation in the radiation characteristics of the star during its contraction. Evaluation of the H109α-line profile yields for DR 21 the unusually high root-mean-square velocity of internal turbulence of 25 kilometers per second, which suggests that this compact HII region is rapidly expanding.

How can OH clouds be located close to the compact HII regions and, like these, be imbedded in a low-density HII region without being destroyed by electron impact or ultraviolet radiation? Reddish's observations are a direct proof that dust exists within HII regions. He concludes that the cocoon is destroyed through contraction to a disk. The OH-emission clouds could be fragments of the cocoon; but it seems that the proximity of OH-emission clouds and compact HII regions should be interpreted more generally as an indication that OH emission occurs preferentially in regions of star-formation. The OH emission could come from protostars that are less massive than O stars. If the formation of all stars in the cluster begins at the same time, less massive stars (which evolve more slowly) will still be protostars when O stars are on the main sequence.

It appears that the radio observations described in this section can give us new insight into the physics of the formation of stars. Further observations, possibly supplemented by 21-centimeter line observations of neutral hydrogen and infrared observations of protostars with low surface brightness temperatures, may eventually enable us to follow a star through its various stages of evolution from a cool and dense cloud of neutral hydrogen to a main-sequence star.

Conclusions and Outlook for Future Observations

At present three types of spectral lines have been detected in the cosmic radio radiation. First to be detected was the 21-centimeter hyperfine structure line that is emitted by clouds of interstellar hydrogen; then four lines, with a wavelength of about 18-centimeters emitted by the OH molecule were discovered. Some of these OH lines are seen in absorption from the same clouds that emit and absorb the 21-centimeter line. On the other hand some OH clouds of very small size, which seem to be associated with regions of star formation and therefore might be protostars, show a strong, nonthermal emission of OH lines. The third, and most recently detected, spectral lines are the recombination lines that are emitted from relatively hot regions of interstellar space, where a large fraction of the atoms are ionized. In contrast to the 21- and the 18-centimeter lines, the recombination lines can be emitted by any atom or ion. In thermodynamic equilibrium the observed line intensities would be proportional to the element abundance and one would hardly expect to observe other than the hydrogen and helium lines. However, as in the case of the line identified as a carbon C109α-line, the radiation of the recombination lines of heavier elements may be greatly enhanced by departures in the population of the energy levels from thermodynamic equilibrium.

In such a rapidly advancing science as radio astronomy, it is always dangerous to assess the present importance of a certain type of observation for the advancement of astrophysics, and even more dangerous to predict its future. The emission of recombination lines seems to be restricted to relatively hot regions of interstellar space where the matter is almost fully ionized; but lines might be emitted from relatively cool regions that are only weakly ionized and therefore are not observed as strong thermal continuum sources. By extending observations of recombination lines to very low frequencies one hopes to detect pressure broadening and hence to determine the actual electron density of HII regions. Comparison of recombination line emission from the millimeter wavelength through the meter wavelength range will help to test improved theories of the statistical equilibrium in HII regions. Further line and continuum surveys, including the southern part of the galaxy, will reveal more about large-scale galactic structure; and, supplemented by other radio astronomical and infrared observations, we may hope to follow the evolution of protostars long before they become visible in the optical range.

Observations of radio recombination lines, and galactic radio astronomy in general, require large fully steerable radio telescopes that can be operated at centimeter wavelengths. There is no doubt that at the moment American radio astronomy is leading in the field of galactic radio astronomy but it is also clear that this leading position is due partly to the fact that centimeter-wave radio telescopes, such as the NRAO 140-foot one, were available for radio astronomers from all parts of the United States as well as from abroad. This lead will soon be contested when radio telescopes of the 100-meter class, now planned or already under construction in Europe, become operational. At present there are no plans for the immediate construction of radio telescopes of similar size in the United States. This could create a dangerous gap in radio astronomical instrumentation and, over a longer period, decrease the quality of radio astronomical research.

References and Notes

1. A. H. Barrett, *Science* **157**, 881 (1967).
2. The star parameters are taken from unpublished papers by R. Hjellming and P. Jarecke, who surveyed theoretical and observational papers pertaining to early-type stars. The Strömgren spheres were computed by R. H. Rubin from a relation obtained by equating the rate of absorption of ionizing photons in the nebula to the rate of emission of Lyman continuum photons from the star, which in turn were obtained from D. Mihalas' [*Astrophys. J. Suppl. Ser.* **9**, 321 (1965)] model stellar atmospheres.

P. G. Mezger, J. Schraml, Y. Terzian, *Astrophys. J.* **150**, 807 (1967).

4. M. Ryle and D. Downes, *ibid.* **148**, L17 (1967).
5. P. G. Mezger, W. Altenhoff, J. Schraml, B. F. Burke, E. C. Reifenstein III, T. L. Wilson, *ibid.* **150**, L157 (1967).
6. K. Davidson and M. Harwit, *ibid.* **148**, 443 (1967).
7. P. Palmer and B. Zuckerman, *Nature* **209**, 1118 (1966).
8. N. S. Kardashev, *Astron. Zh.* **36**, 838 (1959); English translation, *Soviet Astron.-A.J.* **3**, 813 (1960).
9. R. M. Hjellming, P. G. Mezger, J. Schraml, B. F. Burke, in preparation.
10. P. Palmer, in preparation.
11. A. E. Lilley and P. Palmer, *Astrophys. J. Suppl. Ser.*, in press.

12. B. Höglund and P. G. Mezger, *Science* **150**, 339 (1965).
13. P. G. Mezger and A. P. Henderson, *Astrophys. J.* **147**, 471 (1967).
14. P. G. Mezger and B. Höglund, *ibid.*, p. 490.
15. A. E. Lilley, D. H. Menzel, H. Penfield, B. Zuckerman, *Nature* **209**, 468 (1966)
16. L. Goldberg, *Astrophys. J.* **114**, 1225 (1966).
17. H. R. Griem, *ibid.* **148**, 547 (1967).
18. H. Penfield, P. Palmer, B. Zuckerman, *ibid.*, p. L25.
19. N. H. Dieter, *ibid.* **150**, 435 (1967).
20. M. J. Seaton, *Mon. Notic. Roy Astron. Soc.* **127**, 177 (1964).
21. H. Binh-Dy and R. McCarroll, *Astrophys, J.* 149, L27 (1967); J. E. Dyson, *ibid.* **150**, L45 (1967); D. A. Haylor, *ibid.*, in press.
22. P. Palmer, B. Zuckerman, H. Penfield, A. E. Lilley, P. G. Mezger, *Nature* **215**, 40 (1967).
23. L. Goldberg and A. K. Dupree, *ibid.*, p. 41.
24. P. Palmer, B. Zuckerman, H. Penfield, A. E. Lilley, P. G. Mezger, paper presented at American Astronomical Society, 124th meeting, Williams Bay, Wisconsin, June 1967.
25. A. E. Lilley *et al.*, *Nature* **209**, 468 (1966).
26. C. R. O'Dell, M. Peimbert, T. Kinman, *Astrophys. J.* **140**, 119 (1964).
27. J. R. Percy and P. Demarque, *ibid.* **147**, 1200 (1967).
28. P. Palmer, *ibid.* **149**, 715 (1967).
29. B. Zuckerman, P. Palmer, H. Penfield, A. E. Lilley, *ibid.* **149**, L61 (1967).
30. R. X. McGee and F. F. Gardner, *Nature* **213**, 579 (1967).
31. M. A. Gordon and M. L. Meeks, *Astrophys. J.* **149**, L21, (1967).
32. P. G. Mezger, J. Schraml, Y. Terzian, *Astrophys. Lett.*, in press; P. G. Mezger and S. A. Ellis, *ibid.*, in press.
33. G. R. Burbidge, R. J. Gould, and S. R. Pottasch, *Astrophys. J.* **138**, 945 (1963); D. E. Osterbrock, *ibid.* **142**, 1423 (1965).
34. R. M. Hjellming, *ibid.* **143**, 420 (1966).
35. R. H. Rubin, thesis, Case Western Reserve University (1967).
36. M. Peimbert, *Astrophys. J.* **150**, 715 (1967).
37. P. G. Mezger, B. F. Burke, E. C. Reifenstein III, T. L. Wilson, progress reports given at the 124th meeting of the American Astronomical Society, June 1967, and at the 13th meeting of the International Astronomical Union, Prague, September 1967.
38. G. Westerhout, *Bull. Astron. Inst. Neth.* **14**, 215 (1958).
39. W. Altenhoff, P. G. Mezger, H. Wendker, G. Westerhout, *Veröff. Sternwarte Bonn, No. 59*, (1960), p. 48.
40. W. Becker and R. Fenkart, *Z. Astrophys.* **56**, 257 (1963).
41. P. Henderson, thesis, University of Maryland (1967).
42. B. Zuckerman, A. E. Lilley, H. Penfield, *Nature* **208**, 441 (1965).
43. V. C. Reddish, *Mon. Notic. Roy. Astron. Soc.* **135**, 251 (1967).
44. W. Altenhoff, in preparation.
45. National Radio Astronomy Observatory, Green Bank, West Virginia, is operated by Associated Universities, Inc., under contract with the National Science Foundation. The portion of this work carried out at Harvard was supported by the National Science Foundation under grant GP–7337.

Value of Mammalian Cell Culture as a Biochemical Tool

D. Perlman

Until some 20 years ago the techniques of cultivating mammalian cells in vitro remained almost exclusively research projects. To be sure, Harrison (as far back as 1908) and others had demonstrated that animal cells could be maintained for days and months in vitro, and Strangeways and Fell had made the same demonstration for organ culture some 40 years ago. However, the cumbersome technology, the poor definition of physical and chemical requirements, and a general lack of quantitative methods discouraged all but the most painstaking, devoted, and determined investigators. This picture began to change in the 1940's when G. O. Gey and Wilton Earle and their colleagues showed that cells from a variety of tissues could be successfully maintained in vitro through use of rather simple media and careful attention to certain principles. Now, in 1968, these techniques have been so well defined and the complex media and equipment are so readily available from commercial supply houses that many biochemists, microbiologists, pharmacologists, and other biological scientists use mammalian cell culture as a biochemical tool. Their observations on various phenomena have been summarized in hundreds of publications in scientific journals, and it seems timely to consider the value of mammalian cell culture as a tool. What are its strong points and what are its disadvantages? What are the pitfalls that can be avoided? Where will the use of this tool lead us? What new areas may be exploited in the near future?

There are several applications of mammalian cell culture other than those related directly to virology and to cancer research. These include (i) study of mechanisms of cytotoxicity and correlation of the cytotoxicity of drugs with other pharmacological attributes; (ii) study of the biogenesis of hormones and other "vital" products at the cellular level; (iii) determination of nutritional requirements of mammalian cells from "specialized" tissues or cells grown under unusual stresses; and (iv) study of host-parasite relationships at the cellular level. Cell culture has also been used in studying the life cycle of the cell, radiation effects, and nuclear-cytoplasmic interactions, topics which are outside the scope of this article.

Among the various animal cell types that have been cultivated for long or short periods in vitro are epithelial cells, connective cells, cartilage and bone cells, nerve cells, muscle cells, reticular cells from bone marrow, lymph nodes and spleen, and leukocytes from the blood, all of which may be derived from the embryo or the adult. Depending on their origin, some of these cells can be cultivated continuously, whereas others multiply slowly or not at all. For example, leukocyte cultures are, for the most part, short-lived cultures in which there is cell proliferation without a net increase of the cell population. The changes in morphology and function of leukocytes in such cultures is associated with significant biochemical phenomena. This article is confined to an evaluation of the biochemical potential of established cell lines—that is, cells which have been in tissue culture for many generations. These cell lines, although sometimes of heterogeneous population, are readily available to biochemists and other laboratory scientists from a variety of sources, including the American Type Culture Collection and several commercial biological supply houses.

Mechanisms of Cytotoxic Action

In the past 12 years, since Eagle and Foley (*1*) summarized their observations on the cytotoxic action of carcinolytic agents in tissue culture, the action of thousands of chemical compounds and fermentation concentrates has been

The author is professor of pharmaceutical biochemistry, School of Pharmacy, University of Wisconsin, Madison.